

Article

# Effect of Satellite Temporal Resolution on Long-Term Suspended Particulate Matter in Inland Lakes

Zhigang Cao <sup>1,2</sup>, Ronghua Ma <sup>1,3,\*</sup>, Hongtao Duan <sup>1</sup>, Kun Xue <sup>1</sup> and Ming Shen <sup>1,2</sup>

<sup>1</sup> Key Laboratory of Watershed Geographic Sciences, Nanjing Institute of Geography and Limnology, Chinese Academy of Sciences, Nanjing 210008, China; zgcao@niglas.ac.cn (Z.C.); htduan@niglas.ac.cn (H.D.); kxue@niglas.ac.cn (K.X.); mshen@niglas.ac.cn (M.S.)

<sup>2</sup> University of Chinese Academy of Sciences, Beijing 100049, China

<sup>3</sup> Jiangsu Collaborative Innovation Center of Regional Modern Agriculture & Environmental Protection, Huaiyin Normal University, Huai'an 223300, China

\* Correspondence: rhma@niglas.ac.cn; Tel.: +86-025-86882168

Received: 23 October 2019; Accepted: 25 November 2019; Published: 26 November 2019



**Abstract:** The temporal resolution of satellite determines how well remote sensing products represent changes in the lake environments and influences the practical applications by end-users. Here, a resampling method was used to reproduce the suspended particulate matter (SPM) dataset in 43 large lakes (>50 km<sup>2</sup>) on the eastern China plain during 2003–2017 at different temporal resolutions using MODIS Aqua (MODISA) based on Google Earth Engine platform, then to address the impact of temporal resolution on the long-term SPM dataset. Differences between the MODISA-derived and reproduced SPM dataset at longer temporal resolution were higher in the areas with large water dynamics. The spatial and temporal distributions of the differences were driven by unfavorable observation environments during satellite overpasses such as high cloud cover, and rapid changes in water quality, such as water inundation, algae blooms, and macrophytes. Furthermore, the annual mean difference in SPM ranged from 5–10% when the temporal difference was less than 10 d, and the differences in summer and autumn were higher than that of other seasons and surpassed 20% when the temporal resolution was more than 16 d. To assure that difference were less than 10% for long-term satellite-derived SPM datasets, the minimal requirement of temporal resolution should be within 5 d for most of the inland lakes and 3 d for lakes with large changes in water quality. This research can be used to not only evaluate the reliability of historically remote sensing products but also provide a reference for planning field campaigns and applying of high spatial resolution satellite missions to monitor aquatic systems in the future.

**Keywords:** lakes; SPM; Google Earth Engine; revisit time

## 1. Introduction

Lakes are an important component of terrestrial ecosystems and a valuable resource for human survival and development [1,2]. In recent decades, as climate change and human activities have intensified, many lakes have decreased in size and some have even disappeared and with eutrophication being increasingly exacerbated, water quality has deteriorated and lake ecosystems have degraded significantly [3–5]. Due to the change in the lake environment having a progressive process, we must learn from a long-term historical variation of lake environment, so as to understand the process of lake changing and its driving factors. Learning from the history of environmental changes in lakes can enable better control and managements of lakes. Traditionally, long-term water quality monitoring of lakes has depended on field surveys, for example, there is a long-term observation history for Lake Tahoe (USA, 1967–present) [6], Lake Zurich (Switzerland, 1972–present) [7], and Lake Taihu (China,

1992–present) [8]. However, a high observation frequency is difficult to achieve with this method because it is highly time consuming and expensive, therefore satellite remote sensing data has become increasingly important for monitoring lake environments.

For lakes, two types of scientific subjects are mainly observed using remote sensing: Special/extreme environmental events in the lake (e.g., cyanobacterial blooms, river plumes, etc.) [9,10] and long-term spatial-temporal variations of the water environment (e.g., water boundary, water quality, respectively) [11–13]. The former requires a high temporal resolution, while the latter requires a long-term data achieve. In theory, a greater satellite revisit frequency and a longer time series are preferred, however, trade-offs occur in spatial resolution, temporal resolution, radiometric resolution, etc. [14]. Currently, the geostationary satellite instruments can provide hourly observations and meet the requirements for the observations of special events of water quality events (Table 1). However, the short archive, low spatial resolution, and local measurements limit the application of such imagery for long-term observations of global lakes. In fact, the development of a credible long-term water quality dataset has been pursued by environmental and remote sensing communities [15,16]. When using a time series of satellites data to analyze the changes in the water, the remote sensing products are assumed to represent the spatial and temporal variations of the water body itself, thus the higher observation frequency may obtain the more reliable results for water environments.

**Table 1.** The specifics of several common satellite instruments. GSD (m) is ground sample distance.

Instrument	Satellite	Duration	GSD (m)	Revisit Time	Number of Bands
GOCI	COMS	2011–	500	1 h	8
AHI	Himawari 8	2015–	500, 1000, 2000	10 min	1, 3, 2
PMS	GaoFen 4	2016–	50	20 s	5
MODIS	Terra/Aqua	1999–	250, 500, 1000	1 d (0.5 d) <sup>1</sup>	2, 5, 12
VIIRS	NPP/NOAA-20	2011	375,750	1 d	3, 11
OLCI	Sentinel 3 A/B	2016–	300	3 d	21
MSI	Sentinel 2 A/B	2015–	10,20,60	10 d (5 d) <sup>1</sup>	12
OLI	Landsat 8	2013–	30	16 d	7
ETM+	Landsat 7	1999–	30	16 d	6
WV	GF-1/2	2013–	30	4 d	4
HRG	SPOT-5	2002–	2.5	26 d	6

<sup>1</sup> When two satellites were used for joint-observation, the revisit time of MODIS and MSI is 0.5 d and 5 d, respectively.

Ocean color instruments (Table 1) with a revisit time of 1–3 d have been widely used to observe the lake environments and build a dataset with approximately 20 years of data such as for algal blooms, chlorophyll-a (Chl<sub>a</sub>), cyanobacteria, suspended particulate matter (SPM), water clarity, and particulate organic carbon. However, ocean color instruments only observe large lakes or reservoirs due to the coarse spatial resolution (300 m–1000 m), and they cannot be used to measure the lake environment before 2000. Therefore, satellite remote sensing data designed for land application (e.g., Landsat, SPOT, and Sentinel-2), which have higher spatial resolution and longer data series, must be employed [17]. Actually, these data have been used to investigate the spatial and temporal variations of inland lake environments, such as algal blooms, macrophytes, water clarity, SPM, and chromophoric dissolved organic matter (CDOM) [4,18–20]. However, the temporal resolutions of these satellite data are low. Satellites capture a transient signal for water flow and the reliability of the annual and monthly mean remote sensed products derived from so few images may be questioned. Moreover, whether the long-term datasets of water quality such as the Landsat series of instruments are credible and the length of temporal resolution required to obtain reliable remote sensing products in inland lakes must be determined. Barnes and Hu [21] showed that their cross-sensor difference in the monthly mean products could reach <10% for a given location only when both MODISA and SeaWiFs provided >15 valid observations per month in the open Gulf of Mexico. However, to the best of our knowledge,

no systematic research has analyzed the impacts of temporal resolution on long-term remote sensing products in inland lakes to date.

The goal of this study is to quantify the effect of satellite temporal resolution on long-term water quality products and determine the requirement of temporal resolution for generating a reliable long-term dataset of water quality in inland lakes. Specifically, the aims of this study are to (1) obtain the long-term SPM satellite products at various temporal resolutions from 2003–2017 using a resampling method; (2) to analyze the impacts of temporal resolution on the spatiotemporal distributions of SPM and elucidate the driving factors; (3) propose a criterion for a minimal temporal resolution for the development of long-term water quality products; and (4) discuss a strategy for monitoring inland lakes using high spatial resolution satellite measurements. The results can be used to evaluate the accuracy of historical products and may provide a reference for planning field campaigns and the designing of satellite missions to monitor aquatic systems in the future.

## 2. Materials and Methods

### 2.1. Study Area

The spatial resolution of MODIS Aqua (MODISA) in the first seven bands is 250 m and 500 m, thus, 43 large subtropical shallow lakes ( $>50 \text{ km}^2$ ) in the middle and lower reaches of the Yangtze River and reach of the Huai River in China ( $28^\circ \text{N}$ – $36^\circ \text{N}$ ,  $111^\circ \text{E}$ – $121^\circ \text{E}$ ) were selected to examine the effect of temporal resolution (Figure 1a). These lakes are subtropical shallow lakes with an average water depth range from 1.1 to 8.4 m, a Chl<sub>a</sub> range from 0.55–240  $\mu\text{g/L}$  (Mean  $\pm$  STD.:  $50.72 \pm 49.94 \mu\text{g/L}$ ), a SPM range from 1.39–170.42 mg/L ( $34.96 \pm 55.99 \text{ mg/L}$ ), and absorption coefficient of CDOM at 443 nm ranges from 0.89–5.04  $\text{m}^{-1}$  ( $0.89 \pm 0.69 \text{ m}^{-1}$ ) [22]. These lakes include those lakes linked to the rivers, eutrophic lakes, and turbid lakes. Typically, the frequent occurrence of cyanobacteria blooms in Lake Taihu and Chaohu has seriously threatened the safe and healthy drinking of tens of millions of people [4], and dredging activities in Lake Poyang and Lake Hongze have decreased water clarity. Hence, these lakes are complex and the results will be adequately representative of that.

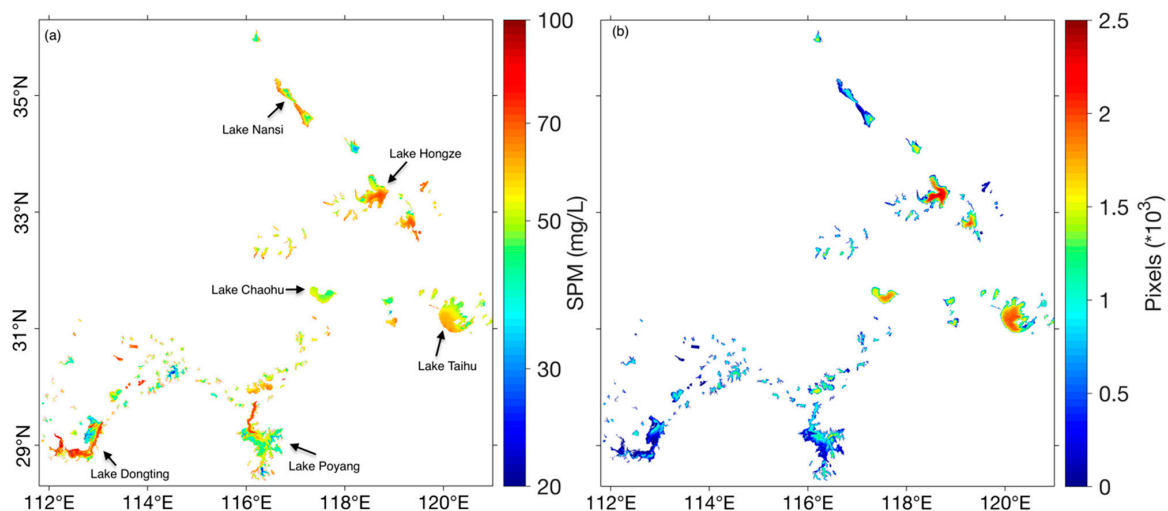


**Figure 1.** The spatial distribution of average MODISA-derived suspended particulate matter (SPM) (a) and total valid pixels (b) in the 43 lakes ( $>50 \text{ km}^2$ ) from 2003 to 2017.

### 2.2. Satellite Data

#### 2.2.1. SPM Products

A published algorithm for SPM estimation was employed to retrieve the SPM of the 43 lakes from 2013–2017 [23]. The algorithm was developed using the field SPM and corresponding surface

reflectance of MODISA in the 58 sampled lakes and reservoirs in the reach of Yangtze River. For the generation of long-term SPM data in the study lakes, daily MODISA surface reflectance products (MYD09GA v6) from 2003 to 2017 were used to retrieve the lakes' SPM. Daily images from MYD09GA data were smoothed using  $7 \times 7$  window in space to minimize the patchiness noise and improve data quality [24]. In addition, the band of Quality Assurance band in MYD09GA was used to mask the pixels potentially contaminated by clouds and cloud shadows, and a threshold segmentation method based on the normalized difference water index (NDWI) was used to extract the water boundaries [25]. Here, only sufficiently large water bodies ( $>50 \text{ km}^2$ ) were used to avoid adjacent land effects. Considering the processing of 15 years of MYD09GA data for such many lakes is very large and time-consuming, all operations were completed using the Google Earth Engine (GEE) platform [26].

### 2.2.2. Cloud Fraction

A total of 180 granules of the MODIS atmosphere monthly global product (MYD08\_M3) from 2003–2017 were downloaded from NASA, which contains monthly  $1^\circ \times 1^\circ$  grid average values of atmospheric parameters, including the atmospheric aerosol particle properties, atmospheric water vapor, and cloud fraction. The cloud fraction will be used to analyze the spatial and temporal differences between the SPM values derived from the different temporal resolutions. The cloud fraction was defined as the ratio between the number of cloudy and probably cloudy pixels and the total number of pixels in each grid cell, and a higher cloud fraction means a higher cloud cover.

### 2.2.3. Water Occurrence and Water Quality Index

The water occurrence, floating algae index (FAI), and cyanobacteria and macrophyte index (CMI) were used to characterize the changes in the lake environments [11,27,28]. Water occurrence was defined as the ratio of water detections and valid observations from January 2003 to December 2017, and a high-water occurrence means a high probability of surface water. FAI was developed to identify floating algae in inland lakes (Equation (1)) and has been widely employed to monitor algal blooms over inland lakes. However, FAI cannot distinguish algal blooms and macrophytes because they all have high FAI values. Therefore, the CMI was developed to distinguish the algal blooms and macrophytes (Equation (2)) and was used together with the FAI [28]. The water covered by macrophytes usually presents high FAI and low CMI, and algal blooms present the opposite pattern. These indices were also calculated using the GEE platform and subsequently were used to analyze the relationships with the SPM variabilities.

$$\text{FAI} = \rho_{859} - (\rho_{645} + (\rho_{1240} - \rho_{645}) \times \frac{\lambda_{859} - \lambda_{645}}{\lambda_{1240} - \lambda_{645}}) \quad (1)$$

$$\text{CMI} = \rho_{555} - (\rho_{469} + (\rho_{1240} - \rho_{469}) \times \frac{\lambda_{555} - \lambda_{469}}{\lambda_{1240} - \lambda_{469}}) \quad (2)$$

where  $\rho_{469}$ ,  $\rho_{555}$ ,  $\rho_{645}$ ,  $\rho_{859}$ , and  $\rho_{1240}$  are the surface reflectance of MYD09GA at 469 nm, 555 nm, 645 nm, 859 nm, and 1240 nm, respectively.

### 2.3. SPM Products at Different Temporal Resolutions

The specifics of different satellites including spatial resolution, temporal resolution, signal-to-noise ratio, and band setting will influence the accuracy of SPM estimations. Thus, it would be hard to analyze the contribution of temporal resolution using the SPM products derived from different satellite measurements. Otherwise, there is no suitable strategy of multi-mission joint observations to generate a long-term SPM dataset in such a large region. Here, we used a group of reproduced datasets of SPM to investigate the effect of temporal resolution. Generally, ocean color instruments that have a temporal resolution of  $\sim 1\text{d}$ , and the remote sensing community that has generally reached a consensus that the water quality parameters derived from these instruments can represent the

spatial and temporal variations of water. Therefore, the daily SPM values derived from MODISA are assumed to be "pseudo-true values" and have been used as the benchmark for long-term remote sensing products. Thus, we reproduced the SPM time-series at different temporal resolutions by resampling daily MODISA-derived SPM from 2003–2017 with different temporal intervals. According to the temporal resolutions of common satellites (e.g., Sentinel 3, Sentinel 2, Landsat, and SPOT series), the intervals of 3 d, 5 d, 8 d, 10 d, 16 d, and 30 d were selected to sample from the time series of the MODIS-derived SPM. These regenerated time-series of SPM corresponded to the SPM dataset of different satellites, for example, the SPM at a 16 d interval represented the Landsat-derived SPM time series. The regenerated data set directly considered observational environments and excluded the impacts of spatial resolutions, signal-to-noise ratios, and band settings from different satellite measurements, so that the complexity of the specific analysis was reduced. It should be noted that the simulation acquired all the data at once on one day by changing the interval (i.e., temporal resolution) and ignored the specific orbit of the satellite, therefore, the regenerated dataset may show an increase or decrease in the number of valid observations compared with the actual observations of a satellite.

The 6 sets of resampled SPM products were compared with the MODISA products, and the unbiased percentage difference (UPD) was calculated (Equation (3)). At the same time, the coefficient of variation (CV, equals to the ratio between standard deviation and mean) of each pixel in the time series was used to characterize the rate of change in water quality. In addition, we also employed the determined coefficient ( $R^2$ ) and root mean square error (RMSE) to evaluate the products differences (Equation (4)).

$$UPD = \frac{1}{N} \sum_{i=1}^N \frac{|x_i - y_i|}{|x_i + y_i|} \times 200\% \quad (3)$$

$$RMSE = \frac{1}{N} \sqrt{\sum_{i=1}^N (x_i - y_i)^2} \quad (4)$$

where  $N$  is the number of point-pairs,  $y_i$  is the predicted value and  $x_i$  is the measured value; here, these parameters are the resampled SPM and MODIS-derived SPM, respectively.

### 3. Results

#### 3.1. SPM Products for Different Temporal Resolutions

Similar to the results of Hou et al., (2017) [23], the average SPM derived from daily MODISA in the 43 large lakes (>50 km<sup>2</sup>) from 2003–2017 was 40–70 mg/L (Figure 1a). Additionally, the number of valid pixels from 2003–2017 showed a distinct pattern (Figure 1b), and the number of valid pixels was greater than 2000 (~36.52%) at approximately 31°N–34°N and less than 1500 (~27.40%) in the lakes in the middle reach of the Yangtze River because of the cloudy and frequent rain in these areas. Also, the number of valid pixels in the peripheral water bodies of Lake Poyang and Lake Dongting was even less than 500 (~9.13%) due to the low water occurrence in winter and spring. Subsequently, the daily MODISA-derived SPM was used to obtain the time series of SPM at different temporal resolutions from 2003–2017 (Figure 2). The SPM concentrations in 43 large lakes presented distinct seasonal variations, with high SPM concentrations in spring and winter and low SPM concentrations in summer and autumn (Figure 2). The SPM resampled by 3 d and 5 d coincided with the MODISA-derived SPM (Figure 2a,b), and temporal variations, including the extreme values, were captured. As temporal resolution of the resampling reduced, the data were generally sparse, and the detail of temporal variation also reduced. For example, some high and low SPM values were not reflected by the regenerated datasets of 16 d and 32 d (Figure 2e,f). Therefore, a longer revisit time will inevitably affect the temporal trend of satellite-derived SPM and subsequently yield increased uncertainty for annual and monthly products.

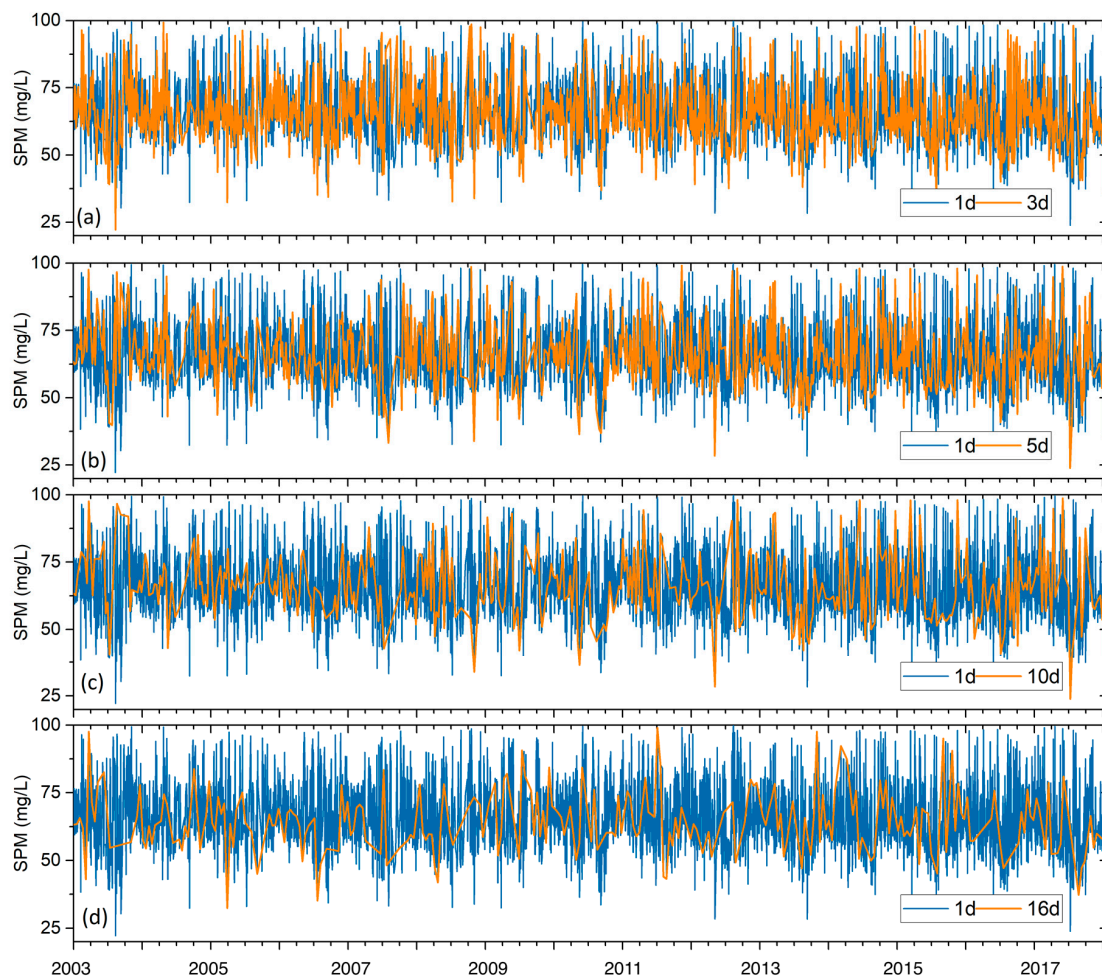


**Figure 2.** Resampled time-series of SPM derived from the satellite instruments at the revisit time 3 d (a), 5 d (b), 10 d (c), 16 d (d) from 2003 to 2017. The blue lines are the SPM time series derived by MODISA (1 d).

### 3.2. Spatial and Temporal Differences in SPM Derived from Different Temporal Resolutions

To quantify the differences in the SPM time series at different temporal resolutions, the UPD between the daily MODISA-derived SPM and regenerated SPM was used for further analysis. Longer temporal resolutions resulted in larger SPM differences and the differences demonstrated a distinct spatial distribution (Figure 3). The UPD of the lakes linking to the Yangtze River was higher and exceeded 10% when the temporal resolution was 3 d however, the UPD in other lakes was low and less than 5% for the temporal resolution of 16 d (e.g., Lake Taihu, Hongze, and Chaohu, Figure 3). For example, there were large differences (more than 10%) in the water bodies surrounding Lake Dongting and Lake Poyang (Zoom A, B, and C areas Figure 3) when the temporal resolution was 3 d or more. While eastern Lake Taihu showed large errors (>8%) (Zoom D, Figure 3), the UPD in most of the water regions was still lower than 5% at a temporal resolution of 16 d. Furthermore, the annual mean difference in SPM was generally within 15% and showed fluctuating variations and the UPD values in 2008, 2010, and 2014 were high and those in 2006, 2009, and 2013 were low (Figure 4a). Moreover, the annual differences increased with the increase in temporal resolution, the UPD ranged from 5–10%, and the annual variation was consistent for the temporal resolutions of 3 d and 5 d. Additionally, the degree of the fluctuation in the annual mean UPD increased as the temporal resolution increased. Moreover, the climatological monthly mean UPD at different temporal resolutions showed a similar seasonal distribution, i.e., UPD values in June to October were higher than those in other months and increased with increasing temporal resolution (Figure 4b). Furthermore, the UPD increased with the

increase in temporal resolution time (Figure 4b), for instance, the monthly mean UPD in summer and autumn was less than 15% for temporal resolutions below 3 d and 5 d and surpassed 20% when the temporal resolution was more than 16 d, while the UPD was less than 5% for all regenerated datasets for the winter and spring.

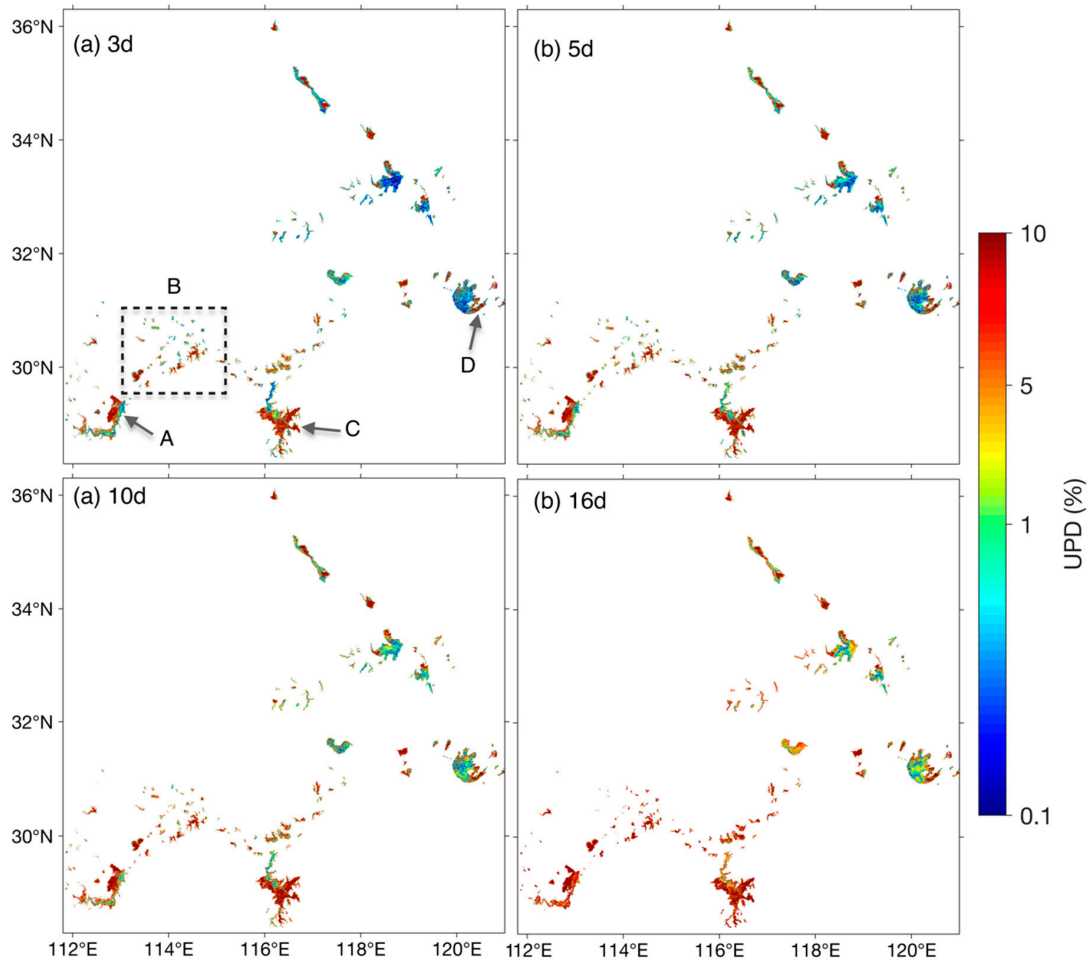


**Figure 3.** (a–d) The difference (UPD: Unbiased percentage difference, %) between MODISA-derived SPM and resampled SPM by revisit time of 3 d, 5 d, 10 d, and 16 d, respectively. Zoom A, B, C, and D represent that the four regions with high UPD values.

### 3.3. Driving Factors of Spatiotemporal Differences for SPM at Different Temporal Resolutions

Recent studies indicated that several unfavorable measurement conditions significantly reduce the quality and quantity of valid ocean color products, with cloud cover, thick aerosols, sun glint, and extreme solar/viewing geometries representing the main reason for missing data from optical instruments [29–31]. Since the solar zenith angle was always less than 60° in our study area, and the view geometry of MODISA can minimize the generation of sun glint, therefore, these conditions will not be discussed here. Overall, the cloud cover in these lakes was 70–80% and showed a significant spatial variability (Figure 5a), where the cloud cover in the areas around Lake Poyang and Lake Dongting (>73%) was higher than that in other areas. Additionally, cloud cover in autumn was lowest (<70%) and that in summer and winter was highest. The cloud cover caused a large amount of missing data and may have led to an increase in the UPD for different temporal resolutions. Indeed, the spatial distributions of UPD was consistent with the cloud cover (Figure 3) and climatological monthly mean UPD was also high in summer (Figure 4b). However, the cloud cover cannot adequately elucidate the temporal differences of UPD in other times, e.g., the low UPD but high cloud cover in winter.

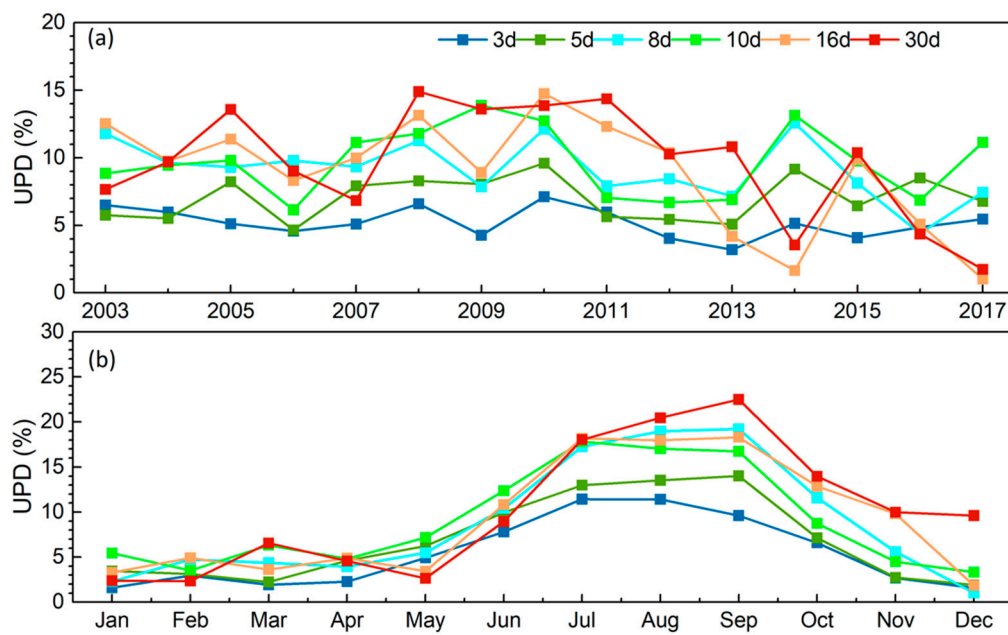


**Figure 4.** The annual (a) and monthly (b) mean UPD (%) between the MODISA-derived SPM and the regenerated SPM at different revisit time from 2003 to 2017.

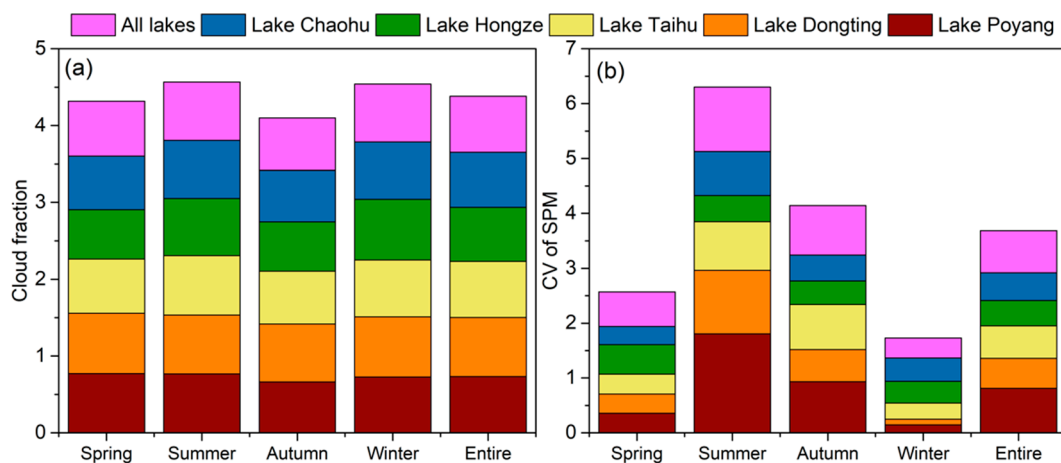


**Figure 5.** The seasonal mean cloud fraction (a) and coefficient of variation (CV) of SPM (b) for the five large lakes and all lakes from 2003 to 2017.

The change in the water itself was also an important factor affecting the spatiotemporal differences in the UPD of the SPM at different temporal resolutions, because rapid changes in the water body require more frequent data to capture specific variations. The CV of the SPM for each pixel from 2003 to 2017 was calculated to reflect the change magnitude in the water body. Furthermore, the water occurrence, FAI, and CMI were used to further address the driving factors of the water changes [11,27,28]. The average CV of SPM was 0.77 and that in the lakes linking to the Yangtze River, particularly in the northwest of Lake Dongting and the peripheral water of Lake Poyang, was higher than 0.85 (Figures 5b and 6a). Eastern Lake Taihu and northern and western Lake Hongze also had higher CV values than other areas (Figure 6a). The areas with high CV values corresponded to the area with a high UPD and can be used to elucidate the spatial differences in UPD of SPM (Figure 6). The high CV in these lakes were induced by the large changes in water inundation and high cover of floating algae and macrophytes (Figure 6b–d). The water occurrence in the lakes linking to the Yangtze River represented by Lake Poyang and Lake Dongting was low from 2003–2017 (Figure 6b), for example, it was as low as 60%

for the peripheral water of Lake Poyang. The high FAI and low CMI values indicated that there was extensive vegetation in the peripheral water of Lake Dongting, Lake Poyang, Eastern Lake Taihu, and Western Lake Hongze [28] (Figure 6c,d). The high FAI and CMI values in the north and west regions of Lake Taihu and west region of Lake Chaohu demonstrated that algal blooms frequently occurred in these areas [4]. Furthermore, the high CV of SPM in summer and autumn caused large differences between the different satellite products (Figure 5), which is consistent with the seasonal distribution of UPD in the SPM (Figures 4 and 5). The high CV of SPM in summer and autumn resulted from high precipitation, macrophytes, and algal blooms [23]. Consequently, the missing data caused by the high cloud cover and the rapid changes in the water itself resulted in the spatiotemporal distributions of the UPD of the SPM at different temporal resolutions.

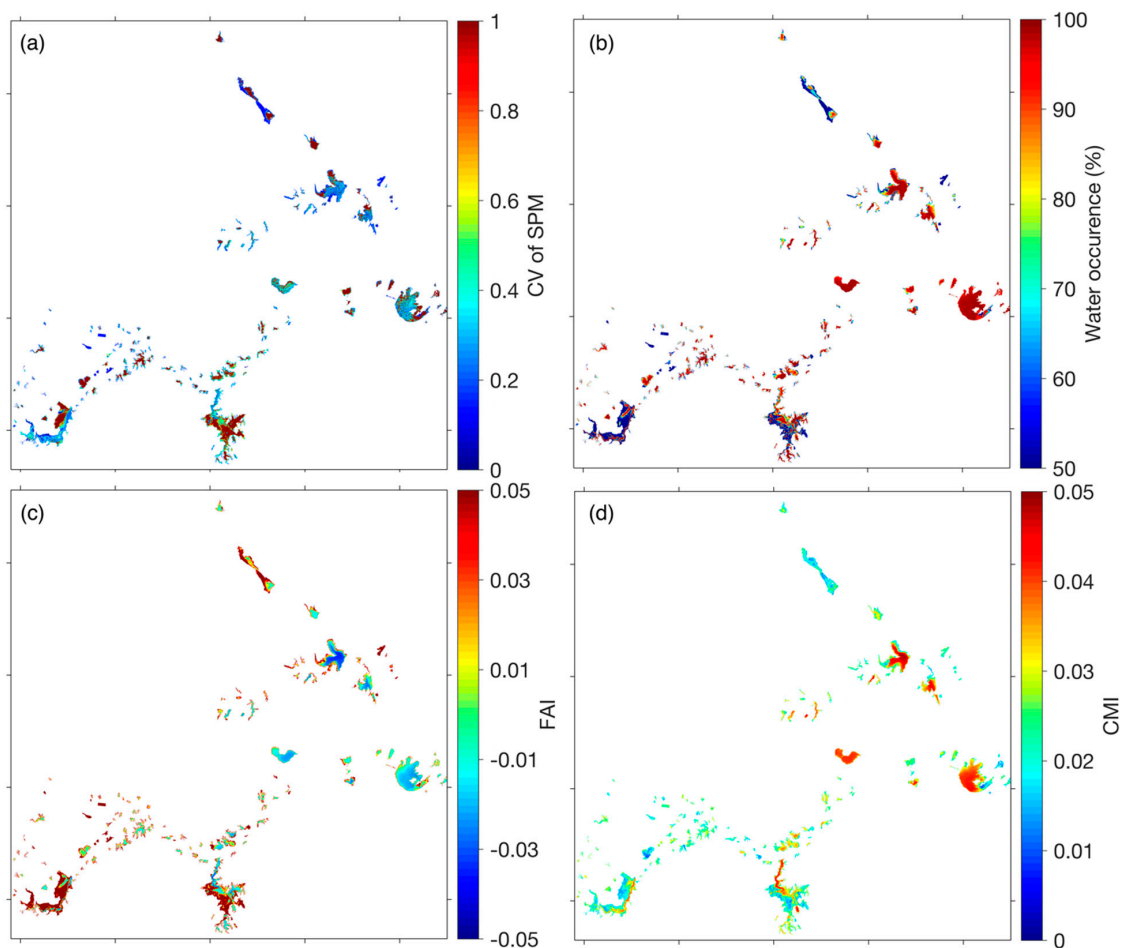


**Figure 6.** (a–d) The spatial distribution of the average CV of SPM, water occurrence, floating algae index (FAI), and cyanobacteria and macrophyte index (CMI) in the eastern lakes of China between 2003 and 2017. The high CV corresponded to a low water occurrence, high FAI, and low CMI, which can reflect the temporal changes in water inundation, algae, and macrophytes.

## 4. Discussion

### 4.1. Accuracy and Uncertainty

Despite that the effect of satellite temporal resolution on the annual and monthly mean SPM has been addressed using the reproduced datasets based on daily MODISA products, uncertainty from the reproduced dataset did exist. First, MYD09GA was originally produced for land observations [32] and it is not an ideal data source for aquatic research because sky scattering and water heterogeneity in atmospheric corrections are not considered and patchiness noise occurs as well [33]. Nevertheless, the

surface reflectance products of MODIS and Landsat has been used to monitor inland waters parameters, such as the SPM, water clarity, and eutrophication status [23,34,35], because such products are low-cost and easily-available and have a certain accuracy at 645 nm and 555 nm. In particular, the  $\rho_{645}/\rho_{555}$  has shown a high accuracy in terms of daily spatial distributions, seasonality, and long-term trends [24], indicating that the SPM retrievals based on the  $\rho_{645}/\rho_{555}$  of MODISA were reliable. Additionally, the performance of empirical algorithm for SPM estimation could be influenced by the constituents and size distribution of particles. For example, the spectral shapes of algae particles and sands differ, and the empirical algorithm may lead to large uncertainties over an area where optical properties exceeded the range of the datasets for developing the algorithm. The SPM algorithm [23] based on the  $\rho_{645}/\rho_{555}$  was developed using data from the tens of lakes located in the middle and lower reaches of the Yangtze River; hence, it was sufficiently representative and could retrieve the reliable long-term SPM datasets in most cases. Although using this model to obtain the SPM in the reaches of the Huai River may lead to uncertainty, the results performed spatiotemporal variations similar to those derived by the local algorithms [12]. Moreover, the 500 m resolution for MYD09GA in 645 nm and 555 nm was insufficient to investigate the medium- and small-sized lakes due to the adjacent land effects [36]. The MODIS surface reflectance of 500 m has been used to study the lake above 25 km<sup>2</sup> [23,34]. To minimize the adjacent land effect and assure the accuracy of the SPM retrieval, only large lakes (>50 km<sup>2</sup>) were used in this study.

Considering that the reproduced dataset based on the time series of the MODIS-derived SPM overlooked spatial resolutions, 40 granules of the Landsat-8 OLI-derived SPM from 2013–2018 for Lake Taihu were compared to the synchronous Terra MODIS-derived SPM (Figure 7). This comparison was expected to elucidate the MODIS-derived SPM and obtain a similar temporal variation to the instrument with a higher spatial resolution in large lakes. Notes that the OLI-derived SPM were retrieved by the same algorithm based on the surface reflectance. The spatial distribution of an averaged SPM derived by MODIS during 2013–2018 was basically consistent with that of OLI (Figure 7a,b), with mean values of  $53.02 \pm 7.03$  mg/L and  $52.30 \pm 8.95$  mg/L, respectively. Although OLI showed more detailed variations of SPM in the lake, their histograms presented similar distributed shapes, indicating that the spatial patterns were the similar (Figure 7c). Moreover, the point-pairs extracted from each image scene in the 300 stations randomly distributed in Lake Taihu for further analysis. To ensure a fair comparison, points covered by cloud, cloud shadow, and with the satellite zenith angle of MODIS less than 60 degree were excluded using the quality-flags band in the products of surface reflectance. To ensure the accordant spatial scale in the sampling, the Chla for each sample was calculated as the mean of the  $3 \times 3$  window of MODIS and the  $50 \times 50$  window for OLI. MODIS- and OLI-derived SPM from 2013–2018 performed a satisfactory consistency and correlation ( $N = 6871$ ,  $R^2 = 0.82$ ,  $RMSE = 3.78$  mg/L, and  $UPD = 7.04\%$ ) (Figure 7d). Notably, MODIS-derived SPM overestimated slightly than that of Landsat-8 due to different band settings. Consequently, the comparison demonstrated that MODIS was able to obtain similar SPM time-series with OLI even if spatial resolutions, operating orbits, and view geometries were different. It should be pointed out that MODIS has insufficient observations on the details of variations in the lake because of its low resolution. If higher spatial resolution satellites were used to investigate the effects of the temporal resolution the subsequent results may have a greater uncertainty (e.g.,  $UPD$ ,  $CV$  of SPM) than that of MODIS because they can observe more details in spatial variations for SPM.

In addition, the assumption that MODISA could obtain reliable water conditions at the 1 d revisit time is the basis of this research. However, water is continually changing. To elucidate the impact of a higher temporal resolution on the results, the GOCI data, which can obtain the eight scenes images from 00:16 to 07:16 UTC every day, were used to validate the MODIS-derived SPM in Lake Taihu. The SPM concentrations were retrieved using the empirical algorithm from the GOCI-derived  $R_{rs}$  by 6SV [37]. Figure 8 showed the spatial distribution of daily mean SPM derived by eight GOCI images, the SPM derived by GOCI, and MODISA at ~5:00 (UTC) on 13 October 2013. Although MODISA slightly overestimated the SPM in central Taihu than GOCI, the MODISA-derived SPM was consistent

with the daily mean SPM of GOCI. Moreover, SPM showed a diurnal variation where the SPM was high in the morning and low in the afternoon (Figure 8d). In fact, the solar radiation in October for Lake Taihu was weak at  $\sim 0$  h and  $\sim 7$  h UTC, which may lead to a considerable uncertainty of SPM estimation in these times. From 01:16 to 06:16 on 13 October 2013, the SPM did not vary significantly and had a  $\sim 15\%$  of the difference with a daily mean SPM. It should be noted that there was an obvious river plume event in Lake Taihu on 13 October 2013. Under such fast-changing water conditions and differences between satellite instruments, the MODISA still obtained a relatively consistent SPM with GOCI, demonstrating that the MODISA-derived SPM could reflect the real variations of SPM in most instances.

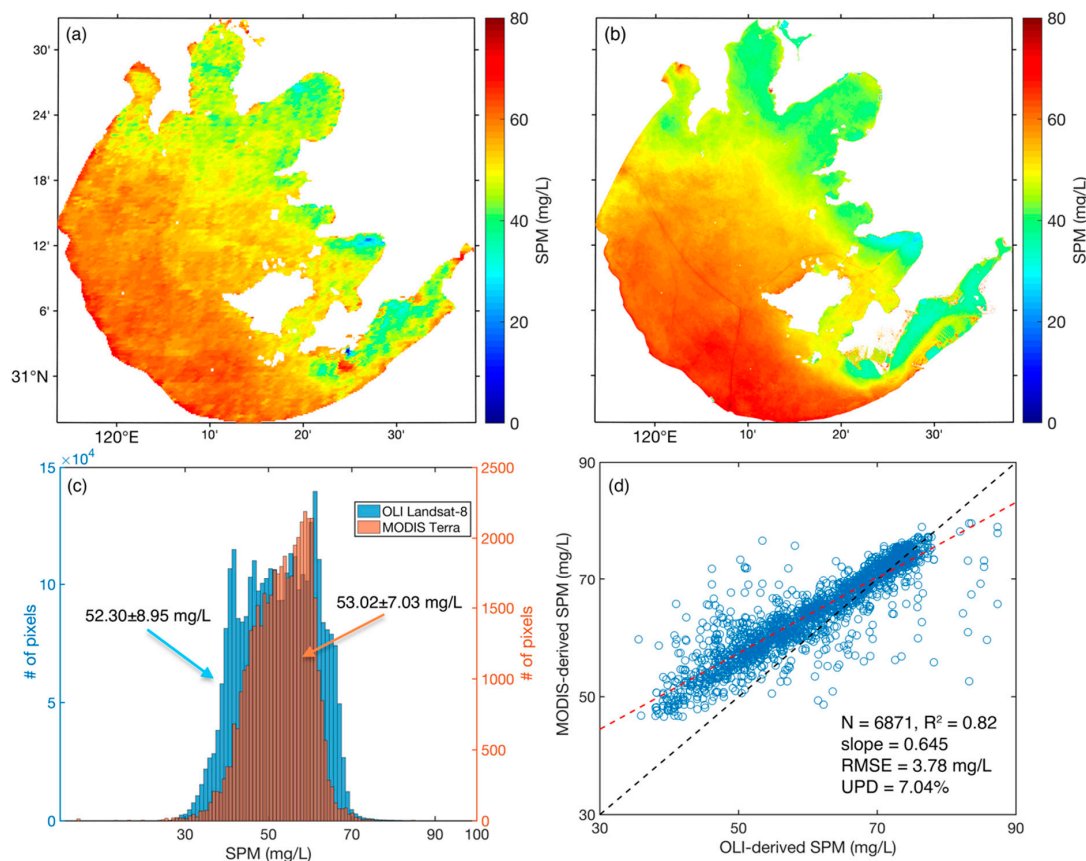


**Figure 7.** Spatial distribution of averaged SPM derived by MODIS Terra (a) and OLI Landsat-8 (b) during 2013–2018. (c) Histograms corresponded to (a) and (b). (d) Scatters of MODIS-derived and OLI-derived SPM extracted from each scene during 2013–2018. For each scene, point-pairs in 300 stations randomly distributed in Lake Taihu were selected and only the data ( $N = 6871$ ) with the Satellite zenith angle of MODIS Terra less than  $60^\circ$  were used to compare here.

Furthermore, our method acquired all the data at once on one day by changing the interval (i.e., temporal resolution) and ignored the specific orbit of the satellite. For example, the global data collected by Landsat 8 was composed of scenes extracted over a period of 16 d. The resampled method may have increased or reduced the number of valid observations compared with the actual observations of the satellite. For example, the high cloud cover, thick aerosol, and sun glint can all reduce the number of valid measurements [21,30,31] thus, the amount of effective data acquired on one day was low and was entered into the regenerated dataset in some areas, resulting in a reduction in the overall number of effective pixels. Hence, the differences in remote sensing products with few valid pixels may increase in these areas [29,30]. The weather during the satellite overpass was random and could not be predicted, however, an equal interval sampling method was employed, which was fair for each pixel. Thus, uncertainty can be seen as systematic.

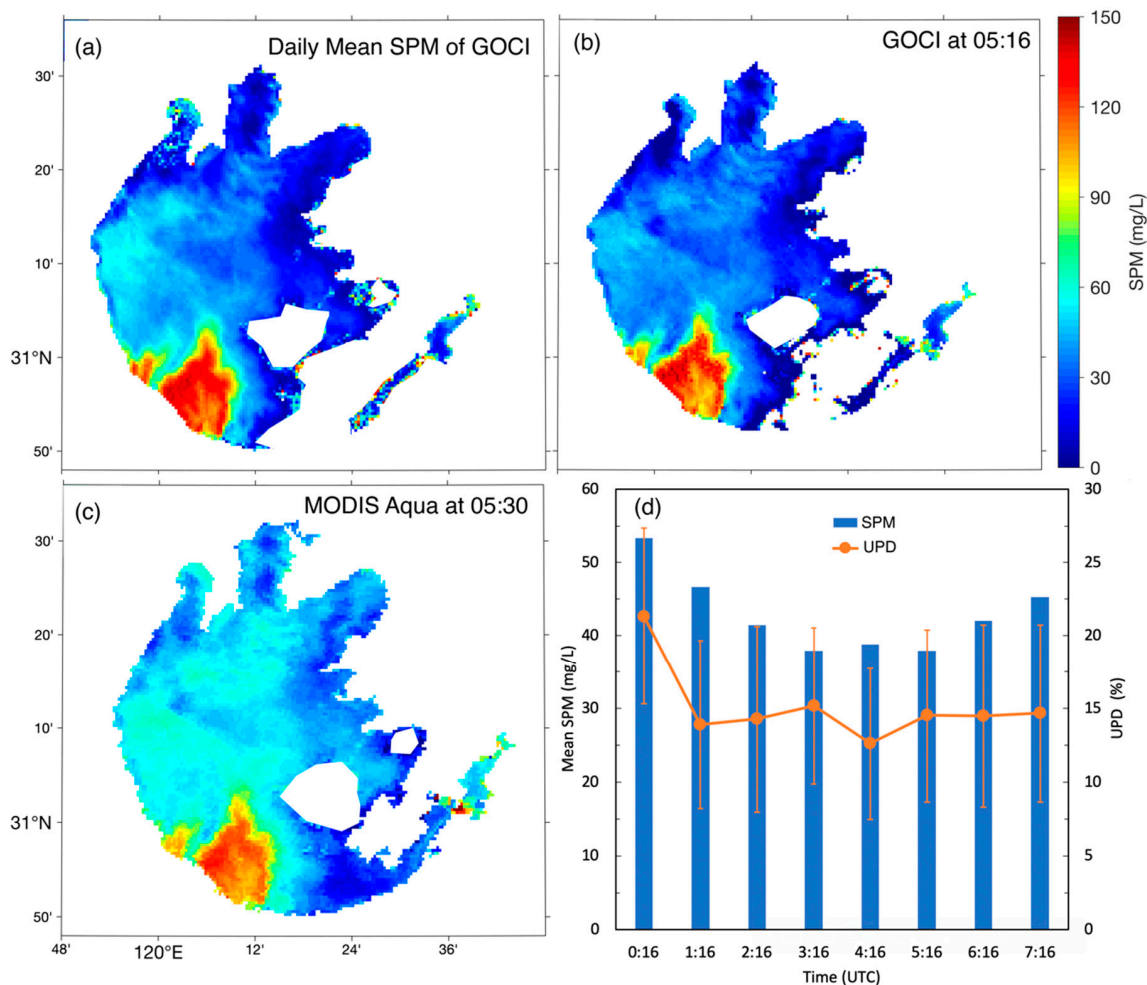


**Figure 8.** (a) Spatial distribution of daily mean SPM estimated by eight scenes from GOCI on 13 October 2013. (b) and (c) was the SPM derived by GOCI and MODISA at ~05:00 UTC, respectively. (d) The mean SPM of each GOCI image on 13 October 2013 and the UPD between the hourly mean SPM and daily mean SPM. Note that most of pixels in Eastern Lake Taihu for the GOCI image were masked due to lower data quality.

#### 4.2. Temporal Resolution Requirements for the Development of Long-Term Quality Water Products

Long-term assessments of the water quality of inland water in response to climate variability and human activities requires consistent long-term observations from multiple sensors [14]. Cloud cover and water quality changes affect the spatiotemporal variations of the UPD at different temporal resolutions hence, long-term water quality datasets require a minimum revisit frequency in different areas and seasons. Barnes and Hu [21] indicated that the number of valid observations required to ensure that MODIS and SeaWiFs were consistent within 10% exceeded 15 per month for their monthly mean Chla data product for multiple  $0.25^\circ$  gridded locations in the Gulf of Mexico. In this research, the annual and climatological monthly mean SPM data were used to determine the minimum temporal resolution requirement in inland lakes. The annual mean UPD was within 10% and increased with increasing temporal resolution (Figures 4a and 9a), and the mean UPD of the 43 lakes dramatically increased when the temporal resolution was longer than 5 d (Figure 4a). For the five largest freshwater lakes in China, due to the extensive changes in water inundation and frequent coverage of wetland vegetation, the UPD in Lake Poyang and Lake Dongting was more than 10% for the temporal resolution of 3 d and even surpassed 100% when the temporal resolution was more than 5 d (Figure 9a). However, the UPD was less than 10% at a temporal resolution of 5 d for Lake Taihu, Hongze, and Chaohu.

The monthly mean UPD was high in Lake Dongting and Lake Poyang, and it was more than 20% at a temporal resolution of 3 d (Figure 9b). The monthly UPDs in the other three lakes were less than 10% and did not change with the temporal resolution. This result indicated that obtaining a reliable annual and monthly mean SPM in most of the lakes required a temporal resolution of at least 5 d (i.e., 73 granules of images per year). The minimum temporal resolution requirement to ensure that the UPD was within 10% in the annual and monthly mean data product generated from the satellite was less than 3 d for lakes with rapid changes in water quality, such as Lake Poyang and Dongting.

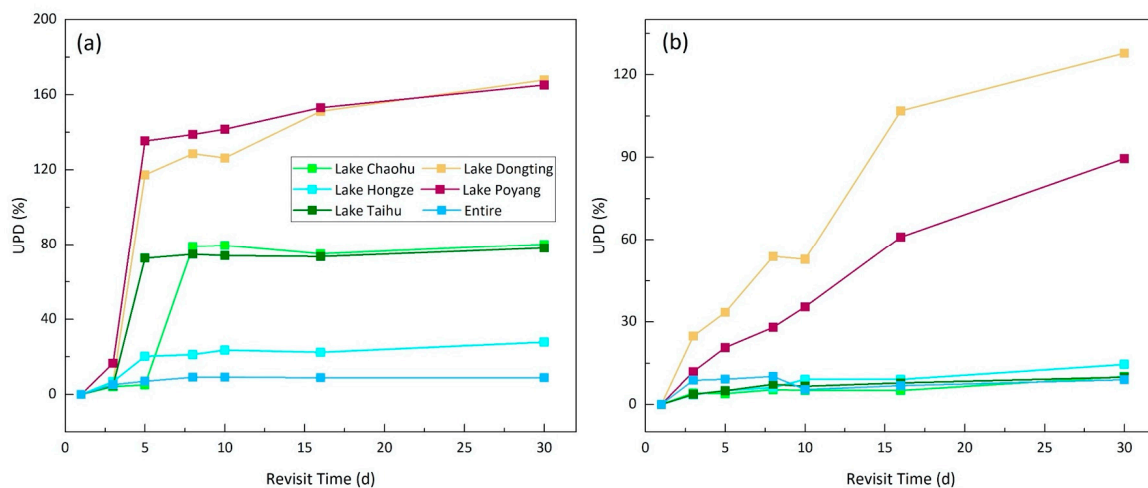


**Figure 9.** Mean UPD (%) for (a) annual and (b) monthly mean SPM as a function of the number of revisit time in Lake Poyang, Lake Dongting, Lake Taihu, Lake Hongze, Lake Chaohu, and all 43 lakes.

Moreover, the trends of the annual and climatological monthly mean SPM values derived from MODISA (1 d), the reproduced Sentinel-2 (A + B) (S2, 5 d), reproduced Landsat-8 (L8, 16 d), and reproduced Sentinel-2 + Landsat-8 (S2 + L8, ~3 d) from 2003–2017 were compared (Figure 10a,b). The annual trends of SPM derived from MODISA, S2, L8, and S2 + L8 showed a significant decrease from 2003 to 2017, and the fitting results for S2 and S2 + L8 were also similar to that of MODISA (Figure 10a). However, the annual mean values of L8 were significantly different in some years (e.g., 2009, 2011, 2016, 2017) compared with other instruments and the annual trends tended to increase. This result indicated that the Landsat products cannot meet the requirement of temporal resolution (5 d) and do not obtain sufficient valid observations. Furthermore, the climatological monthly mean SPM from 2003–2017 were also used to address the spatiotemporal variations of the aquatic system. Although the monthly mean SPM values were low at long temporal resolutions from 2003–2017, all monthly mean SPM values showed consistent variations, including those derived from Landsat (Figure 10b). The climatological monthly method indirectly increased the number of effective observations and reduced the uncertainty of the data, and a longer annual interval increase the reliability of the monthly mean products.

#### 4.3. Implications for the Long-Term Observations of Lakes

For the long-term monitoring of lake water quality worldwide, such as Lake Tahoe (USA, 1967–present) [6], Lake Zurich (Switzerland, 1972–present) [7], and Lake Taihu (China) [8], field surveys were often conducted 1–2 times in each month to collect water quality parameters and analyze the annual and monthly variations of lake environment. For such long observation frequencies, it is important to evaluate whether historical field data can reflect the real variations of the lake environment. Here, the monthly mean SPM and the SPM on the 15th day of every month derived from MODISA from 2003–2017 were compared to elucidate the potential differences (Figure 10c). Noted that the data from the day closest to the 15th were used if it was cloudy on the 15th. There was a significant

difference between the monthly mean SPM and SPM on the 15th, and the SPM in the middle of every month was far from the range of the standard deviation (see the dashed cyan circle in Figure 10c). The SPM on the 15th of each month may capture an extreme water situation and result in deviation caused by using data from one day to represent the month, for example, one day, the extreme rain and strong wind-one day could induce the re-suspension in these shallow lakes and resulted in high SPM [12,38]. The results indicated that the field results of one sampling in a month deviated from the actual situation due to the changes in the water bodies, and the deviation in those lakes with highly dynamic conditions were larger. However, because surveys are time-consuming and expensive, it is not realistic to investigate the water many times every month, therefore remote sensing is a necessary supplement to developing a long-term water environment dataset [39].

Currently, for the large lakes, ocean color instruments with short revisit frequencies, such as MODIS and OLCI, have been used to monitor large lakes or reservoirs via daily observations. However, the monitoring of small lakes requires high spatial resolution instruments, such as Landsat 8 and Sentinel 2 [15,16]. However, the specific satellite sensors must trade-off between spatial resolution and temporal resolution. Landsat 8 and Sentinel 2 A/B have a long temporal resolution, which may cause uncertainty in the annual mean products. In particular, lake monitoring before 2000 depended on only Landsat 5 or SPOT data, and only Landsat 5 is available for free [13,18], therefore, the annual mean water quality products derived from Landsat 5 before 2000 should be carefully considered. In recent years, with the launch of the Landsat 8, Gaofen  $\frac{1}{2}$ , and Sentinel 2A/B satellites, more open source and high-quality imagery data have become available, thus providing an opportunity to improve the temporal resolution of the data through multisensor joint observations. For example, the Landsat-Sentinel-2 virtual constellation has a 2.9 d temporal resolution, and a temporal resolution of <3 d will be readily achieved globally when Landsat 9 becomes operational in early 2021 [40]. Within the next 10–15 years, the OLI onboard Landsat 8/9 and the MSI onboard the Sentinel-2 missions will provide well-calibrated, robust measurements that will enable limnologists, coastal oceanographers, aquatic ecologists, and water resource managers to enhance their monitoring efforts [17,41]. Such frequent temporal resolutions are sufficient to capture dynamical nearshore coastal and inland waters and support a generation of credible long-term water quality datasets. Band design shortcomings and low signal-to-noise ratios are observed for these instruments, however atmospheric corrections are still challenging for inland lakes [42,43]. Thus, further research is required on the accurate estimation of water quality parameters in inland waters to expand the breadth and depth of remote sensing in environmental monitoring application in the future [16].

## 5. Conclusions

Daily surface reflectance products from MODIS Aqua from 2010–2017 were employed to retrieve the SPM of 43 large lakes in the east China plain. These data were used to reproduce datasets at different temporal resolutions based on the Google Earth Engine (GEE) platform. The temporal resolution significantly increased the differences in the annual mean SPM and climatological monthly mean SPM, and the difference showed obvious spatial and seasonal distributions. The cloud cover and temporal change in water quality were the main driving factors underlying the spatiotemporal differences in the SPM derived from measurements with different temporal resolutions. Finally, a 5-day temporal resolution for satellites was proposed as the criterion to develop long-term water quality parameters and obtain credible annual/monthly mean remote sensing products in most of the inland lakes. These results provided theoretical support for remote sensing as an important data source that can supplement in situ surveys in the monitoring of lake environments. As instruments designed for ocean color observations cannot meet the operational requirements of small inland lakes, in the future multi-sensor observations, such as by Landsat 8/9-Sentinel 2A/B for the remote sensing of inland lakes will be needed to cover global lakes every 3 d and provide an opportunity to generate credible water products for small lakes.

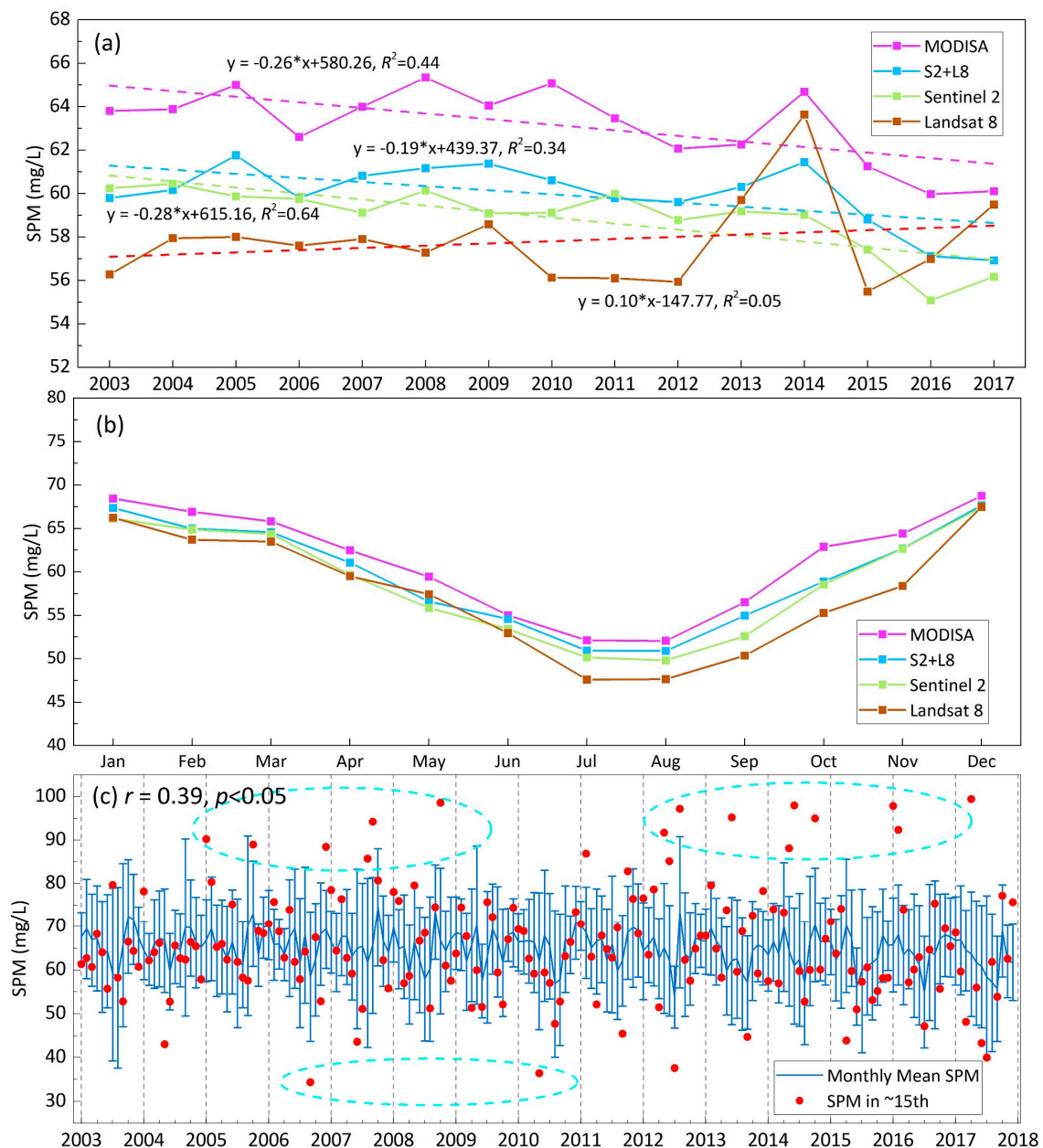


**Figure 10.** The annual (a) and climatological monthly (b) trends of SPM derived from MODIS Aqua, regenerated-Sentinel 2, regenerated-Landsat 8, and regenerated-harmonized datasets of Landsat 8 and Sentinel-2 in large lakes in Eastern China from 2003–2017. The dashed lines were the results of a regression. (c) The variations in annual and monthly SPM and SPM derived from data collected on the 15th of each month, and the dashed cyan circles represent the abnormal values away from the monthly value. Notes that  $r$  is the Pearson correlation coefficient between the monthly mean SPM and SPM in each mid-each month.

**Author Contributions:** Conceptualization, R.M. and Z.C.; Data curation, Z.C. and M.S.; Formal analysis, Z.C., K.X. and H.D.; Funding acquisition, R.M. and H.D.; Methodology, Z.C. and H.D.; Project administration, R.M.; Software, Z.G. and R.M.; Supervision, R.M.; Validation, H.D.; Writing—original draft, Z.C.; Writing—review & editing, Z.C., R.M., H.D., K.X., and M.S.

**Funding:** This research was funded by the National Natural Science Foundation of China (grant number 41431176, 41671358, 41771366), the NIGLAS Cross-functional Innovation Teams (grant number NIGLAS2016TD01) and the program of China Scholarship Council (201904910725).

**Acknowledgments:** The authors would like to thank NASA for providing satellite data and to thank Google Inc. for their processing software platform. The processing codes used in this study are available by email (zhigang0312@gmail.com). We also thank the three anonymous reviewers for their suggestions for this manuscript.

**Conflicts of Interest:** The authors declare no conflict of interest.

## References

1. Johnson, N.; Revenga, C.; Echeverria, J. Managing Water for People and Nature. *Science* **2001**, *292*, 1071–1072. [[CrossRef](#)]
2. Downing, J.A.; Prairie, Y.T.; Cole, J.J.; Duarte, C.M.; Tranvik, L.J.; Striegl, R.G.; McDowell, W.H.; Kortelainen, P.; Caraco, N.F.; Melack, J.M.; et al. The global abundance and size distribution of lakes, ponds, and impoundments. *Limnol. Oceanogr.* **2006**, *51*, 2388–2397. [[CrossRef](#)]
3. Adrian, R.; Reilly, C.M.O.; Zagarese, H.; Baines, S.B.; Hessen, D.O.; Keller, W.; Livingstone, D.M.; Sommaruga, R.; Straile, D.; Van Donk, E. Lakes as sentinels of climate change. *Limnol. Oceanogr.* **2009**, *54*, 2283–2297. [[CrossRef](#)] [[PubMed](#)]
4. Duan, H.; Ma, R.; Xu, X.; Kong, F.; Zhang, S.; Kong, W.; Hao, J.; Shang, L. Two-Decade Reconstruction of Algal Blooms in China's Lake Taihu. *Environ. Sci. Technol.* **2009**, *43*, 3522–3528. [[CrossRef](#)] [[PubMed](#)]
5. Pham, S.V.; Leavitt, P.R.; McGowan, S.; Peres-Neto, P. Spatial variability of climate and land-use effects on lakes of the northern Great Plains. *Limnol. Oceanogr.* **2008**, *53*, 728–742. [[CrossRef](#)]
6. Jassby, A.D.; Reuter, J.E.; Goldman, C.R. Determining long-term water quality change in the presence of climate variability: Lake Tahoe (U.S.A.). *Can. J. Fish. Aquat. Sci.* **2003**, *60*, 1452–1461. [[CrossRef](#)]
7. Posch, T.; Köster, O.; Salcher, M.M.; Pernthaler, J. Harmful filamentous cyanobacteria favoured by reduced water turnover with lake warming. *Nat. Clim. Chang.* **2012**, *2*, 809. [[CrossRef](#)]
8. Qin, B.; Paerl, H.W.; Brookes, J.D.; Liu, J.; Jeppesen, E.; Zhu, G.; Zhang, Y.; Xu, H.; Shi, K.; Deng, J. Why Lake Taihu continues to be plagued with cyanobacterial blooms through 10 years (2007–2017) efforts. *Sci. Bull.* **2019**, *64*, 354–356. [[CrossRef](#)]
9. Chen, X.; Shang, S.; Lee, Z.; Qi, L.; Yan, J.; Li, Y. High-frequency observation of floating algae from AHI on Himawari-8. *Remote Sens. Environ.* **2019**, *227*, 151–161. [[CrossRef](#)]
10. Doxaran, D.; Lamquin, N.; Park, Y.-J.; Mazeran, C.; Ryu, J.-H.; Wang, M.; Poteau, A. Retrieval of the seawater reflectance for suspended solids monitoring in the East China Sea using MODIS, MERIS and GOCI satellite data. *Remote Sens. Environ.* **2014**, *146*, 36–48. [[CrossRef](#)]
11. Pekel, J.F.; Cottam, A.; Gorelick, N.; Belward, A.S. High-resolution mapping of global surface water and its long-term changes. *Nature* **2016**, *540*, 418–422. [[CrossRef](#)] [[PubMed](#)]
12. Cao, Z.G.; Duan, H.T.; Feng, L.; Ma, R.H.; Xue, K. Climate- and human-induced changes in suspended particulate matter over Lake Hongze on short and long timescales. *Remote Sens. Environ.* **2017**, *192*, 98–113. [[CrossRef](#)]
13. Olmanson, L.G.; Brezonik, P.L.; Bauer, M.E. Remote Sensing for Regional Lake Water Quality Assessment: Capabilities and Limitations of Current and Upcoming Satellite Systems. In *Advances in Watershed Science and Assessment*; Younos, T., Parece, T.E., Eds.; Springer International Publishing: Cham, Switzerland, 2015; pp. 111–140. [[CrossRef](#)]
14. International Ocean-Colour Coordinating Group (IOCCG). *Earth Observations in Support of Global Water Quality Monitoring*; International Ocean-Colour Coordinating Group: Dartmouth, NS, Canada, 2018.
15. Palmer, S.C.J.; Kutser, T.; Hunter, P.D. Remote sensing of inland waters: Challenges, progress and future directions. *Remote Sens. Environ.* **2015**, *157*, 1–8. [[CrossRef](#)]
16. Mouw, C.B.; Greb, S.; Aurin, D.; DiGiacomo, P.M.; Lee, Z.; Twardowski, M.; Binding, C.; Hu, C.M.; Ma, R.H.; Moore, T.; et al. Aquatic color radiometry remote sensing of coastal and inland waters: Challenges and recommendations for future satellite missions. *Remote Sens. Environ.* **2015**, *160*, 15–30. [[CrossRef](#)]
17. Pahlevan, N.; Chittimalli, S.K.; Balasubramanian, S.V.; Vellucci, V. Sentinel-2/Landsat-8 product consistency and implications for monitoring aquatic systems. *Remote Sens. Environ.* **2019**, *220*, 19–29. [[CrossRef](#)]
18. Dekker, A.G.; Vos, R.J.; Peters, S.W.M. Analytical algorithms for lake water TSM estimation for retrospective analyses of TM and SPOT sensor data. *Int. J. Remote Sens.* **2010**, *23*, 15–35. [[CrossRef](#)]
19. Pahlevan, N.; Balasubramanian, S.; Sarkar, S.; Franz, B. Toward Long-Term Aquatic Science Products from Heritage Landsat Missions. *Remote Sens.* **2018**, *10*, 1337. [[CrossRef](#)]

20. Olmanson, L.G.; Bauer, M.E.; Brezonik, P.L. A 20-year Landsat water clarity census of Minnesota's 10,000 lakes. *Remote Sens. Environ.* **2008**, *112*, 4086–4097. [[CrossRef](#)]
21. Barnes, B.B.; Hu, C. Cross-Sensor Continuity of Satellite-Derived Water Clarity in the Gulf of Mexico: Insights Into Temporal Aliasing and Implications for Long-Term Water Clarity Assessment. *IEEE Trans. Geosci. Remote Sens.* **2015**, *53*, 1761–1772. [[CrossRef](#)]
22. Xue, K.; Ma, R.H.; Duan, H.T.; Shen, M.; Boss, E.; Cao, Z.G. Inversion of inherent optical properties in optically complex waters using sentinel-3A/OLCI images: A case study using China's three largest freshwater lakes. *Remote Sens. Environ.* **2019**, *225*, 328–346. [[CrossRef](#)]
23. Hou, X.; Feng, L.; Duan, H.; Chen, X.; Sun, D.; Shi, K. Fifteen-year monitoring of the turbidity dynamics in large lakes and reservoirs in the middle and lower basin of the Yangtze River, China. *Remote Sens. Environ.* **2017**, *190*, 107–121. [[CrossRef](#)]
24. Feng, L.; Hu, C.; Li, J. Can MODIS Land Reflectance Products be Used for Estuarine and Inland Waters? *Water Resour. Res.* **2018**, *54*, 3583–3601. [[CrossRef](#)]
25. Li, J.; Sheng, Y. An automated scheme for glacial lake dynamics mapping using Landsat imagery and digital elevation models: A case study in the Himalayas. *Int. J. Remote Sens.* **2012**, *33*, 5194–5213. [[CrossRef](#)]
26. Gorelick, N.; Hancher, M.; Dixon, M.; Ilyushchenko, S.; Thau, D.; Moore, R. Google Earth Engine: Planetary-scale geospatial analysis for everyone. *Remote Sens. Environ.* **2017**, *202*, 18–27. [[CrossRef](#)]
27. Hu, C.M. A novel ocean color index to detect floating algae in the global oceans. *Remote Sens. Environ.* **2009**, *113*, 2118–2129. [[CrossRef](#)]
28. Liang, Q.; Zhang, Y.; Ma, R.; Loiselle, S.; Li, J.; Hu, M. A MODIS-Based Novel Method to Distinguish Surface Cyanobacterial Scums and Aquatic Macrophytes in Lake Taihu. *Remote Sens.* **2017**, *9*, 133. [[CrossRef](#)]
29. Maritorena, S.; d'Andon, O.H.F.; Mangin, A.; Siegel, D.A. Merged satellite ocean color data products using a bio-optical model: Characteristics, benefits and issues. *Remote Sens. Environ.* **2010**, *114*, 1791–1804. [[CrossRef](#)]
30. Feng, L.; Hu, C. Comparison of Valid Ocean Observations Between MODIS Terra and Aqua Over the Global Oceans. *IEEE Trans. Geosci. Remote Sens.* **2016**, *54*, 1575–1585. [[CrossRef](#)]
31. Gregg, W.W.; Casey, N.W. Sampling biases in MODIS and SeaWiFS ocean chlorophyll data. *Remote Sens. Environ.* **2007**, *111*, 25–35. [[CrossRef](#)]
32. Kaufman, Y.J.; Tanré, D. Algorithm for remote sensing of tropospheric aerosol from MODIS. *NASA MODIS Algorithm Theor. Basis Doc. Goddard Space Flight Cent.* **1998**, *85*, 3–68.
33. Shenglei, W.; Junsheng, L.; Bing, Z.; Qian, S.; Fangfang, Z.; Zhaoyi, L. A simple correction method for the MODIS surface reflectance product over typical inland waters in China. *Int. J. Remote Sens.* **2016**, *37*, 6076–6096. [[CrossRef](#)]
34. Wang, S.; Li, J.; Zhang, B.; Spyrakos, E.; Tyler, A.N.; Shen, Q.; Zhang, F.; Kuster, T.; Lehmann, M.K.; Wu, Y.; et al. Trophic state assessment of global inland waters using a MODIS-derived Forel-Ule index. *Remote Sens. Environ.* **2018**, *217*, 444–460. [[CrossRef](#)]
35. Kuhn, C.; de Matos Valerio, A.; Ward, N.; Loken, L.; Sawakuchi, H.O.; Kampel, M.; Richey, J.; Stadler, P.; Crawford, J.; Striegl, R.; et al. Performance of Landsat-8 and Sentinel-2 surface reflectance products for river remote sensing retrievals of chlorophyll-a and turbidity. *Remote Sens. Environ.* **2019**, *224*, 104–118. [[CrossRef](#)]
36. Olmanson, L.G.; Brezonik, P.L.; Bauer, M.E. Evaluation of medium to low resolution satellite imagery for regional lake water quality assessments. *Water Resour. Res.* **2011**, *47*. [[CrossRef](#)]
37. Xu, Y.; Qin, B.; Zhu, G.; Zhang, Y.; Shi, K.; Li, Y.; Shi, Y.; Chen, L. High Temporal Resolution Monitoring of Suspended Matter Changes from GOCI Measurements in Lake Taihu. *Remote Sens.* **2019**, *11*, 985. [[CrossRef](#)]
38. Zhang, Y.; Shi, K.; Zhou, Y.; Liu, X.; Qin, B. Monitoring the river plume induced by heavy rainfall events in large, shallow, Lake Taihu using MODIS 250 m imagery. *Remote Sens. Environ.* **2016**, *173*, 109–121. [[CrossRef](#)]
39. Roughgarden, J.; Running, S.W.; Matson, P.A. What Does Remote Sensing Do For Ecology? *Ecology* **1991**, *72*, 1918–1922. [[CrossRef](#)]
40. Li, J.; Roy, D.P. A Global Analysis of Sentinel-2A, Sentinel-2B and Landsat-8 Data Revisit Intervals and Implications for Terrestrial Monitoring. *Remote Sens.* **2017**, *9*, 902. [[CrossRef](#)]
41. Wulder, M.A.; Loveland, T.R.; Roy, D.P.; Crawford, C.J.; Masek, J.G.; Woodcock, C.E.; Allen, R.G.; Anderson, M.C.; Belward, A.S.; Cohen, W.B.; et al. Current status of Landsat program, science, and applications. *Remote Sens. Environ.* **2019**, *225*, 127–147. [[CrossRef](#)]

42. Schott, J.R.; Gerace, A.; Woodcock, C.E.; Wang, S.X.; Zhu, Z.; Wynne, R.H.; Blinn, C.E. The impact of improved signal-to-noise ratios on algorithm performance: Case studies for Landsat class instruments. *Remote Sens. Environ.* **2016**, *185*, 37–45. [[CrossRef](#)]
43. Ruddick, K.; Vanhellemont, Q.; Dogliotti, A.; Nechad, B.; Pringle, N.; Zande, D.V.d. New opportunities and challenges for high resolution remote sensing of water colour. In Proceedings of the Ocean Optics XXIII, Victoria, BC, Canada, 23–28 October 2016.



© 2019 by the authors. Licensee MDPI, Basel, Switzerland. This article is an open access article distributed under the terms and conditions of the Creative Commons Attribution (CC BY) license (<http://creativecommons.org/licenses/by/4.0/>).